Inorg. Chem. **2007**, *46*, 2187–2192

Rare-Earth Metal-Rich Antimonides: Syntheses, Structures, and Properties of Tm_3Sb and Lu_7Sb_3

Shalabh Gupta,[†] Ling Chen,[‡] Ashok K. Ganguli,*[,†] and John D. Corbett*

Department of Chemistry, Iowa State University, Ames, Iowa 50011

Received October 10, 2006

The two most metal-rich lanthanide antimony phases known were obtained from high-temperature solid state syntheses, that for Tm_3Sb being of greater difficulty because of its apparent incongruent melting. The Tm_3Sb phase crystallizes in the tetragonal space group $P4_2/n$ (No. 86) with a Ti_3P-type (Pearson: tP32) structure, a = 12.2294(5) Å, c = 5.9852(5) Å, and Z = 8. The phase Lu_7Sb_3 exhibits a Sc_7As_3-type tetragonal structure, $I4/mcm$ (No. 140) (tI56), with a = 15.5974(7) Å, c = 8.8130(7) Å, and Z = 8. Both structures are described in terms of compact arrays of condensed chains of metal polyhedra (tetrahedral, tetrahedral star, trigonal prismatic, cubic) together with six- to nine-coordinate Sb in metal polyhedra. Magnetic susceptibility data on the paramagnetic Tm_3Sb are also reported.

Introduction

The plethora of new metal-rich compounds that have come to the forefront in recent years reveal the remarkable and almost innumerable ways in which the component atoms can bond and arrange themselves in periodic solids. Among these, metal-rich pnictides, chalcogenides, and halides of the electron-poorer transition metals have provided a large number of remarkable examples.[1−6] The newest and least precedented new compounds and structures are often found for the *lanthanide* (Ln) elements or, with inclusion of the group 3 elements Sc−La, what are collectively termed the *rare-earth* metals (R).

Among the basic structural features of these metal-rich derivatives are highly condensed metal polyhedra such as octahedra or trigonal prisms which are often linked directly or through the intervening anions into chains, layers, or 3D arrays. A great diversity of bonding is witnessed in such compounds, ranging from overriding metal−metal bonding and, usually, metallic properties to significant covalency between the electropositive and electronegative components. In this regard, the metal richness of the compounds is often measured by the metal/nonmetal element ratio which is in many interesting cases large enough to not only ensure formal reduction of the anion but also leave valence electrons for M−M interactions. We report here the syntheses and structural refinements of the first two binary lanthanide antimonides that are more reduced than Ln_2Sb, namely, Tm_3Sb and Lu_7Sb_3.

Although the Ti_3P structure type of the first is widely known among the phosphides, arsenides, silicides, stannides, and germanides of Ti, Zr, Hf, Nb, and Ta,[7] the occurrence of trivalent metals in this structure type has been reported only for Y_3Sb and that according to an assignment of powder diffraction data.[8] (The 1990 report of Lu_3Sb[9] is not considered creditable—see the Results and Discussion section.) The new Lu_7Te_3 compound represents only the second example of the Sc_7As_3 structure type that was reported by Berger and co-workers in 1981 without much detail.[10] These two examples come from new explorations of metal-rich Ln−

* To whom correspondence should be addressed. E-mail: jcorbett@iastate.edu (J.D.C.), ashok@chemistry.iitd.ernet.in (A.K.G.).
[†] Department of Chemistry, Indian Institute of Technology, New Delhi 110016, India.
[‡] Fujian Institute of Research on the Structure of Matter, CAS, Fuzhou, Fujian 350002, P. R. China.

(1) Franzen, H. F. *Prog. Solid State Chem.* **1978**, *12*, 1.
(2) Simon, A. *Angew. Chem., Int. Ed. Engl.* **1981**, *20*, 1.
(3) Hughbanks, T. R. *J. Alloys Compd.* **1995**, *229*, 40.
(4) Kleinke, H. *Chem. Soc. Rev.* **2000**, *29*, 411.
(5) Corbett, J. D. *Inorg. Chem.* **2000**, *39*, 5178.
(6) Corbett, J. D. In *Inorganic Chemistry in Focus II*; Meyer, G., Naumann, D., Wesemann, L., Eds.; Wiley-VCF: New York, 2005; Vol 2, Chapter 8.
(7) Villars, P.; Calvert, L. D. *Pearson's Handbook of Crystallographic Data for Intermetallic Phases*, 2nd ed.; American Society for Metals: Metals Park, OH, 1991.
(8) Schmidt, F. A.; McMasters, O. D. *J. Less-Common Met.* **1970**, *21*, 415.
(9) Abdusalyamova, M. N.; Faslyeva, N. D.; Eliseev, A. A.; Shishkin, E. A.; Rakhmatov, O. I.; Chuiko, A. G.; Shumakova, T. P. *J. Less-Common Met.* **1990**, *166*, 229.
(10) Berger, R.; Nolaeng, B.I.; Tergenius, L.-E. *Acta Chem. Scand. A* **1981**, *35*, 679.

10.1021/ic0619409 CCC: $37.00
Published on Web 02/16/2007

Sb systems driven not only by the belief that the antimonides may afford useful thermoelectric materials but also by the thought that such novelties as recently uncovered in other antimony systems, viz., $A_2Ca_{10}Sb_9$,[11] $Mg_{5.23}Sm_{0.77}Sb_4$,[12] and Lu_6MoSb_2,[13] and the very unusual metal-rich lutetium compounds of the neighboring tellurium[6] may be found.

Experimental Section

Syntheses. Single crystals of the title compounds were obtained following high-temperature reactions of mixtures of the high-purity elements Tm or Lu pieces (99.95%, Ames Laboratory) and Sb chunks (99.99%, Johnson-Matthey) in $^1/_4$ in. diameter Nb tubing welded under an Ar atmosphere. (Ta is not as satisfactory with Sb.[11]) The tubes were further jacketed in evacuated and sealed silica containers and heated in resistance furnaces.

The Tm_3Sb phase was eventually obtained in >95% yield (plus <5% of an unknown phase represented by a line near $\theta = 32°$) from a reaction of that composition that was first quenched from 1050 °C after a 3 day equilibration. The quenched product was then annealed at 400 °C for 7 days prior to cooling at 3 °C/h. Prior reactions had shown that quench and anneal at 600 °C alone were not suitable. In addition, other reaction conditions did not give good yields of the target phase: (a) fast cooling (100 °C/h) from 1250 °C to room temperature, (b) intermediate annealing at 700 or 400 °C, or (c) slow cooling alone to 800 or 600 °C. These behaviors suggest that Tm_3Sb undergoes a peritectic formation/decomposition reaction at relatively low temperatures, as bounded above. On the other hand, metal-rich compositions Pr_xSb reacted in parallel with those of Tm_xSb gave no evidence for the analogous Pr_3Sb phase, yielding only Pr_2Sb[14] plus a few extra powder pattern lines.

Explorations in the metal-rich region of the Lu−Sb system indicated that two new phases were formed according to the Guinier powder patterns of the products of various reactions. In particular, samples with Lu/Sb molar proportions of 3:1 and 11:4 (compare to $Lu_{11}Te_4$[15]) were first arc-melted with losses of <1.3 wt %. The two products either without or with subsequent annealing in Ta at 1200 °C for ~1 day all yielded powder patterns that contained ~90% of the pattern of what turned out to be the title phase of Lu_7Sb_3. The results suggest that this phase melts congruently or very nearly so. Well-shaped crystals came from the last of the four reaction products, the 11:4 sample after annealing. On the other hand, somewhat Sb-richer reactions yielded the novel Lu_6MoSb_2 (a site-occupancy variant of Fe_2P type) after annealing through incorporation of some Mo from the protective foil used to wrap the arc-melted buttons.[13]

Powder X-ray Diffraction. Powder diffraction data were recorded at ~22 °C on a Huber 670 Guinier camera equipped with an area detector and Cu Kα radiation ($\lambda = 1.540598$ Å). The investigations were carried out on samples held between two Mylar sheets with the help of a little Apiezon grease and mounted on the twin-ring assembly inside the glovebox. The presence of each title phase was established by visual comparison of the observed pattern with that generated from the lattice parameters, space group, and the atomic positions subsequently determined from a single-crystal study. Impurity detection is estimated to be of the order of 5% in terms of equivalent scattering.

Table 1. Some Crystal and Structural Refinement Parameters for Tm_3Sb and Lu_7Sb_3

empirical formula	Tm_3Sb	Lu_7Sb_3
fw	628.54	1590.0
cryst syst	tetragonal	tetragonal
unit cell dimens		
$a = b$, Å	12.2294(5)	15.5974(7)
c	5.9852(5)	8.8130(7)
V, Å^3	895.14(9)	2144.0(2)
space group, Z	$P4_2/n$ (No. 86), 8	$I4/mcm$ (No. 140), 8
density (calcd) (Mg/m^3)	9.328	9.852
abs coeff (Mo Kα), mm^{-1}	64.63	71.14
final indices:		
R1, wR2[a] [$I > 2\sigma(I)$]	0.0274, 0.0506	0.0180, 0.0304
(all data)	0.0323, 0.0518	0.0257, 0.0314

[a] $R1 = \Sigma(|F_o - F_c|)/\Sigma(|F_0|)$, $wR2 = [\Sigma w(F_o^2 - F_c^2)/\Sigma wF_o^4]^{1/2}$.

Single-Crystal Studies. Selected single crystals were mounted in thin-walled capillaries inside a glove box designed for crystal mounting and then examined on a Bruker APEX diffractometer equipped with a CCD detector, a graphite monochromator, and a Mo Kα fine-focus sealed tube ($\lambda = 0.71073$ Å). Three sets of 606 frames of data were collected at room temperature for Tm_3Sb with a scan width of 0.3° in ω and an exposure time of 10 s per frame. The reflection intensities were integrated with the SAINT subprogram in the SMART software package[16] using a narrow-frame integration algorithm. The integration of the data for the indicated tetragonal unit cell yielded a total of 7462 reflections to a maximum θ angle of 28.20° (0.75 Å resolution), of which 1079 were observed ($I > 2\sigma(I)$) and independent (completeness = 97.9%, $R_{int} = 5.07\%$). Empirical absorption corrections were made using the multiscan technique with the SADABS program.[16] Space group determination by the XPREP program in the SHELXTL 6.1 software package[17] suggested $P4_2/n$ (No. 86) or *Imma* (No. 74) on the basis of systematic absences, and the mean value of $\langle E^2 - 1 \rangle$ (0.839) suggested that the structure is centrosymmetric and in the former. No systematic absence violations or inconsistent equivalents were observed. All four independent atoms were located with SHELXS using direct methods, and the structure was refined anisotropically (38 variables) with the aid of SHELXTL 6.1 and full-matrix least-squares on F_o^2 for all reflections to give convergence at R1 = 2.74%, wR2 = 5.06% for $I > 2\sigma(I)$ data and 3.23 and 5.18% for all data, respectively. The largest residual peaks were 1.632 and −1.800 e·Å^{-3}.

The solution of the crystal structure of Lu_7Sb_3 took place in a closely parallel manner. A sphere of data in reciprocal space to $2\theta = 56.32°$ was collected from the best specimen with 10 s/frame exposures. The tetragonal space group $I4/mcm$ (No. 140) was strongly indicated, and the structure was readily solved therein by direct methods and refined without problem with the aid of SHELXTL. Absorption was corrected with the aid of the SADABS routine to give 736 observed reflections ($I > 2\sigma(I)$, $R_{int} = 0.0589$). The final anisotropic refinement with seven independent atoms and 33 variables converged at R1 = 0.0180, ωR2 = 0.0304 for $I > 2\sigma(I)$ data. This also yielded quite uniform displacement ellipsoids except for U_{33} of Lu5 which was a little larger (2:1) normal to the plane of its four nearest neighbors (see Discussion). The largest ΔF residuals were 1.46 and −1.27 e·Å^3, both <2 Å from Lu atoms. Some crystal and refinement data for both studies are collected in Table 1.

Magnetic Susceptibilities. Data for Tm_3Sb were measured at fields of 1 and 3 T over a range of 6−300 K with the aid of a

(11) Ganguli, A. K.; Gupta, S.; Corbett, J. D. *Inorg. Chem.* **2006**, *45*, 196.
(12) Gupta, S.; Ganguli, A. K.; Corbett, J. D. *Inorg. Chem.* **2006**, *45*, 8175.
(13) **(**13**)** Chen, L.; Corbett, J. D. *Inorg. Chem.* **2004**, *43*, 436.
(14) Abdusalyamova, M. N.; Rakhmatov, O. L.; Faslyeva, N. D.; Tchuikw, A. G. *J. Less-Common Met.* **1988**, *141*, L23.
(15) Chen, L.; Xia, S.-Q.; Corbett, J. D. *Inorg. Chem.* **2005**, *44*, 3057.
(16) *SMART*; Bruker AXS, Inc.: Madison, WI, 1996.
(17) *SHELXTL*; Bruker AXS, Inc.: Madison, WI, 2000.

Table 2. Atomic Coordinates ($\times 10^5$) and Equivalent Isotropic Displacement Parameters ($Å^2 \times 10^4$) for Tm_3Sb[a]

	Wyckoff	*x*	*y*	*z*	*U* (eq)
Tm1	8*g*	15022(4)	66109(4)	22406(7)	58(1)
Tm2	8*g*	53039(4)	7346(4)	25739(7)	50(1)
Tm3	8*g*	10960(4)	22328(4)	51580(7)	54(1)
Sb1	8*g*	4872(5)	20968(5)	1202(11)	50(2)

[a] *U* (eq) is defined as one-third of the trace of the orthogonalized U^{ij} tensor.

Table 3. Bond Lengths (Å) in Tm_3Sb

Tm(1)−Tm(1)	3.2689(9)	Tm(2)−Tm(3)	3.5591(6)
Tm(1)−Tm(1)	3.7813(4)	Tm(3)−Tm(3)	3.4956(9)
Tm(1)−Tm(2)	3.4058(7)	Tm(3)−Tm(3)	3.7375(8)
Tm(1)−Tm(2)	3.5956(7)	Tm(1)−Sb(1)	3.0996(8)
Tm(1)−Tm(2)	3.6257(6)	Tm(1)−Sb(1)	3.2269(8)
Tm(1)−Tm(2)	3.7399(7)	Tm(2)−Sb(1)	3.0599(8)
Tm(1)−Tm(3)	3.7173(7)	Tm(2)−Sb(1)	3.1822(8)
Tm(1)−Tm(3)	3.8105(7)	Tm(2)−Sb(1)	3.2583(8)
Tm(2)−Tm(2)	3.4950(9)	Tm(3)−Sb(1)	3.0496(8)
Tm(2)−Tm(2)	3.6432(9)	Tm(3)−Sb(1)	3.0664(8)
Tm(2)−Tm(3)	3.3915(6)	Tm(3)−Sb(1)	3.0772(8)
Tm(2)−Tm(3)	3.5345(6)	Tm(3)−Sb(1)	3.1103(8)

Quantum Design (MPMS) SQUID magnetometer. The weighed sample was held between two fused silica rods within a tightly fitting outer silica tube, and the assembly was sealed under helium.[18] The raw data were corrected for the susceptibility of the container and the diamagnetic contributions of the ion cores.[19]

Results and Discussion

The new Tm_3Sb and Lu_7Sb_3 phases represent the first lanthanide examples of these stoichiometries, the first structural refinement of any Ti_3P-type R_3Sb, and the first confirmation of the singular structure reported for the rather distant Sc_7Sb_3. The syntheses of these two new lanthanide antimonides turned out to be very different in their facilities (Experimental Section). Tm_3Sb was secured in good yield after an (assumed) melt of that composition had been quenched and then annealed for a week at ∼ 400 °C (but not as high as 600 °C), presumably because the Tm_3Sb melts low and quite incongruently. On the other hand, Lu_7Te_3 was obtained in high yield from compositions in its neighborhood following either arc melting or subsequent annealing of the melted product at 1200 °C for about 1 day.

Tm_3Sb. The tetragonal structure of Tm_3Sb ($P4_2/n$), the first rare-earth metal example for which this structure type has been quantified, is of a Ti_3P generic classification,[20] a lower symmetry member of a sizable class of A_3B-type phases.[21] Positional and distance data are collected in Tables 2 and 3. As shown explicitly in Figure 1 in an infinite ∼-[010] view, the antimony (vice P) resides in a somewhat distorted tetrakaidecahedron (better known as a tricapped trigonal prism), with Tm−Sb distances in a moderately narrow range of 3.05−3.26 Å. However, this description neglects the significant and distinctive roles of the three Tm atom types, as shown color-coded in a near-[001] view of

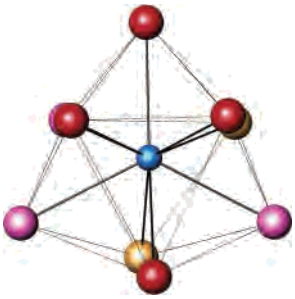

Figure 1. The distorted tricapped trigonal prism of Tm that surrounds each Sb atom in Tm_3Sb (∼[010] infinite perspective). The Tm atoms are color-coded as in Figure 2.

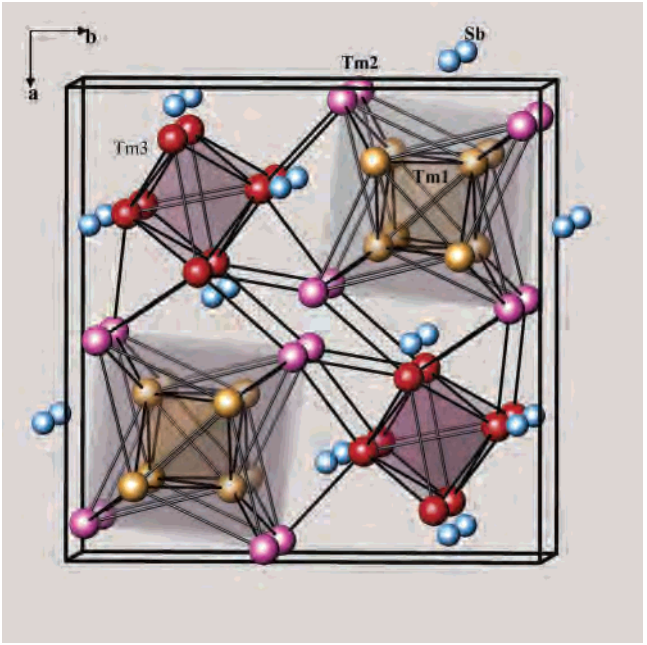

Figure 2. ∼[001] Projection of the structure of tetragonal Tm_3Sb ($P4_2/n$) color-coded by atom number: Tm1, golden (center of tetrahedral star chain); Tm2, orchid (bridging atoms); Tm3, red (tetrahedral chain); Sb, blue. The chains and polyhedra along the $\bar{4}$ axes are highlighted. Tm−Sb bonds are omitted for clarity.

the relatively complex unit cell in Figure 2. A simplified description of the structure follows. The basic metal polyhedra consist of commensurate chains of Tm3 (red) tetrahedra that share opposite edges along the $\bar{4}$ axis at $^1/_4$, $^1/_4$, *z* (top left), etc., plus a parallel chain of shared *tetrahedral star* units built of Tm1 (golden) and Tm2 (orchid) along $^1/_4$, $^3/_4$, *z*, etc. The wider black "bonds" emphasize these features, but the overall array, distorted somewhat because of its complexity, exhibits additional (marked) metal−metal contacts over a range of 3.27−3.89 Å. All the additional Tm−Tm bonds involve the more protruding Tm2 atoms (orchid). In more detail, the two metal chains are generated from Tm3 metal dimers (3.50 Å, red) and from Tm1 dimers (3.27 Å, golden) that are both positioned normal to $\vec{c}$ and alternate by 90° down that axis according to the $\bar{4}$ symmetry. The repeat distances in the simpler red tetrahedral chain so generated alternate between 3.74 and a long 4.03 Å, the latter length included for geometric completeness, whereas these repeats are 3.74 and 3.78 Å in the golden chain of tetrahedra.

(18) Guloy, A. M.; Corbett, J. D. *Inorg. Chem.* **1996**, *35*, 4669.
(19) Selwood, P. In *Magnetochemistry*; Interscience Publishers: New York, 1956.
(20) Lundstrom, T.; Snell, P.-O. *Acta Chem. Scand.* **1967**, *21*, 1343.
(21) Hyde, B. G.; Andersson, S. *Inorganic Crystal Structures*; John Wiley & Sons: New York, 1989; pp 360−370.

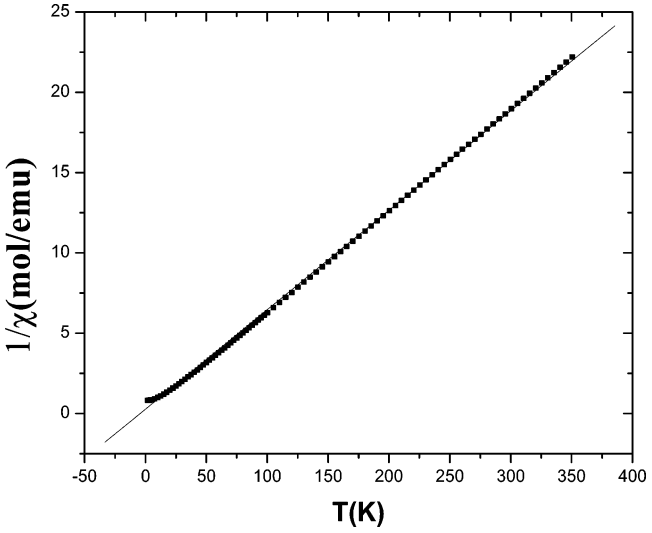

Figure 3. Curie−Weiss plot of inverse susceptibility vs temperature (K) at 1 T for Tm_3Sb.

The tetrahedral star description for the latter results because all facing pairs of triangular faces on the chain of Tm1 tetrahedra are capped by Tm2 atoms (orchid) to generate a second larger and inverted chain of tetrahedra. (These Tm2−Tm1 distances range between 3.40−3.60 Å to the vertices and 3.74−3.89 Å to atoms in the shared Tm1−Tm1 edges.) (This tetrahedral star construction is a common feature in intermetallic structures.[22]) The Tm2 atoms also bridge edges or bond exo to atoms in the simpler red chain at 3.39−3.56 Å. (A complete equivalent to Figure 2 with distances marked is given in the Supporting Information, Figure S1.) Finally, although it is not very clear in this figure, the Sb atoms (blue) lie between the metal chains, being positioned at the same level in *z* and side-on to each type of dimer, and achieve moderately regular 9-fold bonding to all Tm atoms (marked in Figure 1). A view of this $SbTm_9$ polyhedron with the same orientation as in Figure 2 and enumerated distances is given in the Supporting Information, Figure S2.

Magnetic Properties. Molar magnetic susceptibilities of powdered Tm_3Sb crystals were measured over the temperature range of 2−350 K. Figure 3 shows that the variation of the inverse magnetic susceptibility as function of temperature can be well fit to a Curie−Weiss relation over substantially the entire temperature range (Weiss $\Theta = 4.2$ K). The calculated spin-only moment over the entire temperature region is 6.56 μ_B per Tm atom. This value is somewhat smaller than the theoretically predicted moment of Tm^{3+}, 7.56 μ_B. The apparent reduction in the moment can probably be attributed to a small impurity content or orbital quenching, although a high magnetic anisotropy of Tm ions[23] or the presence of some Tm^{2+} with a smaller moment ($4f^{13}$) in this well-reduced metallic phase cannot be eliminated.[24] A small decrease in the magnetic susceptibility below 5 K may signal the onset of short-range antiferromagnetic order, as also indicated by the magnetization curves at 2 and 300 K given in the Supporting Information, Table S3. There is no suggestion of such a localized state in the structure, however.

Lu_7Sb_3. An 1990 study of the Lu−Sb phase diagram via DTA and powder pattern data concluded the existence of only Lu_3Sb and Lu_5Sb_3 in this region.[9] However, the new lines in their X-ray powder data were evidently used only for qualitative evidence as no structural assignment for the metal-richer phase was noted. However, the ease and directness with which we obtained high yields of only Lu_7Sb_3 and free metal (judging from Guinier powder patterns) from compositions with Lu/Sb proportions of 3.0 and 2.75 (Experimental Section) strongly suggest that the earlier association of an Lu_3Sb composition with an incongruent 1290 °C melting point must be in error. (According to their phase diagram this marked the decomposition of Lu_3Sb(s) into ~Lu_5Sb(l) plus Lu_5Sb_3(s).) (An incongruent melting point of 1240 °C has been reported for Y_3Sb.[8]) Lu_2Sb may be a reasonable alternative for their powder pattern data, although substantial contamination may have also been present inasmuch as the thermal analysis samples in this composition region were held in fused silica containers and heated as high as 1600−1700 °C.

The only previous report of this structure type came from a 1981 single-crystal diffractometer study of the parent Sc_7As_3.[10] Its synthesis, which started with the elements in a silica container and was followed by arc-melting and a brief annealing at 1200 °C by induction heating, evidently gave a quite low yield. The structure was largely described in comparative qualitative terms. Our synthetic explorations of the Lu−Sb and related systems, with the great advantage of Ta containers, have revealed that a number of new phases are formed.[6]

A summary of some crystallographic data for Lu_7Sb_3 is given in Table 1, and the atom positional and distance data are collected in Tables 4 and 5. Figure 4 shows the tetragonal structure (*I*4/*mcm*) viewed down the short (8.8 Å) *c*-axis with three types of polyhedra highlighted to give a better understanding of the results. The Lu atoms are represented by red-brown spheres and the Sb atoms by yellow spheres. Bonds are shown for *d* (Lu−Sb) < 3.20 Å and for *d* (Lu−Lu) < 3.40 Å, generally to not obscure the construction, although values of the latter up to 3.45 Å or higher are probably also important in this relatively condensed structure. The three colored polyhedra shown mark those about Sb1 and Sb2, green and brown, and the metal-rich $(La2)_8$ around Lu4 as a pale blue cube, respectively. In addition, fairly obvious square planar Sb1 atoms about Lu5 at $0,0,{}^1/_4$, ${}^1/_2,{}^1/_2,{}^1/_4$, etc. define another polyhedral array, and a cube of bridging Lu3 around this can also be included (below). These polyhedra are all intercondensed via shared atoms, as shown.

Metal polyhedra about the antimony "glue" atoms provide the principal interconnections in the structure via shared Lu atoms. The Lu atoms in the unusual (green) polyhedra about seven-coordinate Sb1 are shared with three like units about a central Lu5 as well as with the brown (Sb2) and blue (Lu4)

(22) Häussermann, U.; Svensson, C.; Liden, S. *J. Am. Chem. Soc.* **1998**, *120*, 3867.
(23) Cooper, B. R.; Vogt, O. *Phys. Rev B* **1970**, *1*, 1211.
(24) Lawrence, J.M.; Riseboroughs, P. S.; Parks, R. D. *Rep. Prog. Phys.* **1981**, *44*, 1.

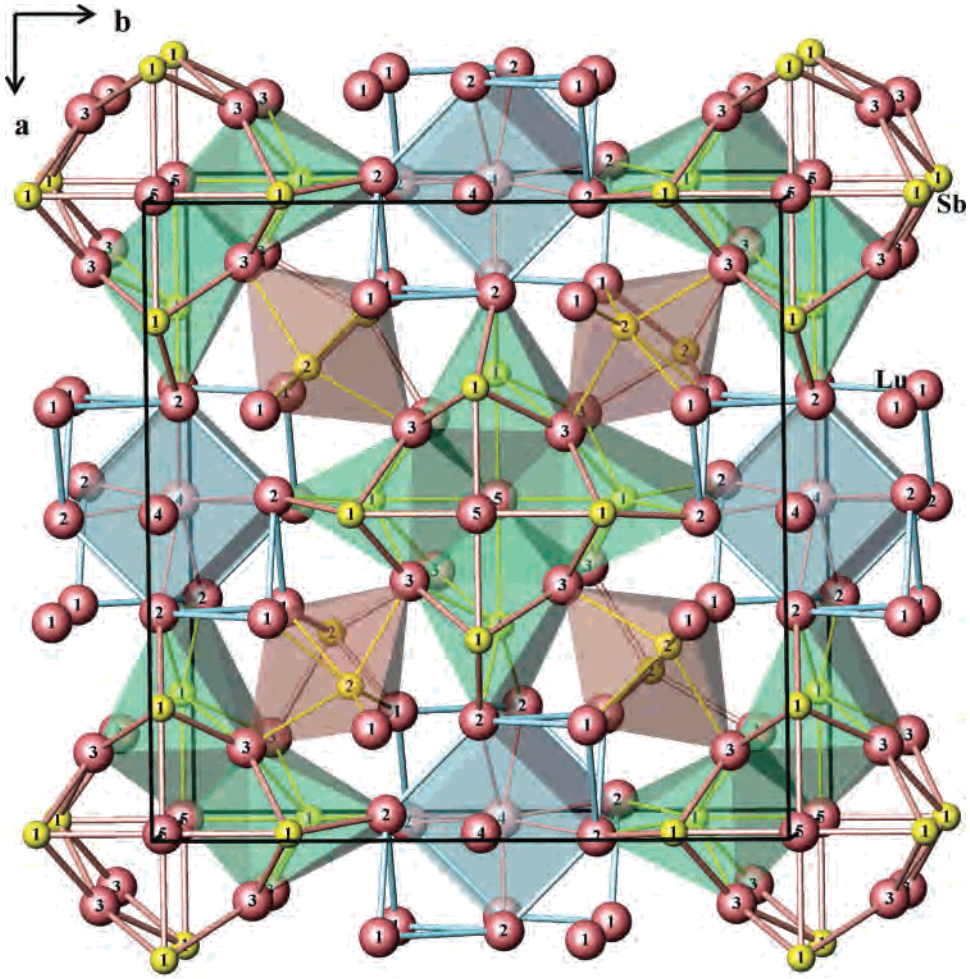

Figure 4. ~[001] Projection of the tetragonal crystal structure of Lu_7Sb_3 (*I*4/*mcm*) with the Lu (red-brown) and Sb (yellow) atoms as spheres. The colored polyhedra are centered by Sb1 (green), Sb2 (brown), and Lu4 (light blue).

Table 4. Atomic Coordinates ($\times 10^5$) and Equivalent Isotropic Displacement Parameters ($Å^2 \times 10^4$) for Lu_7Sb_3[a]

atom	Wyckoff	*x*	*y*	*z*	*U* (eq)
Lu1	16*l*	16 558(2)	66 558(2)	19 423(5)	115(1)
Lu2	16*k*	1729(3)	3495(3)	0	114(1)
Lu3	16*k*	12 355(3)	11 670(3)	0	121(2)
Lu4	4*b*	0	$^1/_2$	$^1/_4$	120(2)
Lu5	4*a*	0	0	$^1/_4$	118(2)
Sb1	16*j*	19 752(4)	0	$^1/_4$	107(1)
Sb2	8*h*	71 946(4)	21 946(4)	0	118(2)

[a] *U* (eq) is defined as one-third of the trace of the orthogonalized U^{ij} tensor.

Table 5. Bond Lengths (Å) in Lu_7Sb_3

Lu(1)−Sb(2)	3.9452(6)	Lu(3)−Sb(2)	2.9611(5)
Lu(1)−Sb(2)	3.0596(9)	Lu(3)−Sb(2) × 2	3.0820(4)
Lu(1)−Lu(2) × 2	3.3265(5)	Lu(3)−Sb(2) × 2	3.1870(4)
Lu(1)−Sb(1) × 2	3.3869(4)	Lu(3)−Lu(5)	3.4469(4)
Lu(1)−Lu(1)	3.4235(9)	Lu(3)−Lu(3) × 2	3.7488(6)
Lu(1)−Lu(2) × 2	3.5512(5)	Lu(3)−Lu(3)	3.7488(6)
Lu(1)−Lu(4)	3.6852(5)	Lu(3)−Lu(1)	3.7854(5)
Lu(1)−Lu(3) × 2	3.7854(5)	Lu(3)−Lu(2)	3.7861(7)
Lu(2)−Sb(1) × 2	3.0857(5)	Lu(5)−Sb(1) × 4	3.0808(7)
Lu(2)−Lu(2)	3.2593(8)	Lu(5)−Lu(3) × 8	3.4469(4)
Lu(2)−Sb(2)	3.265 (1)	Sb(2)−Lu(1)	2.9452(6)
Lu(2)−Lu(1) × 2	3.3265(5)	Sb(2)−Lu(3) × 2	2.9611(5)
Lu(2)−Lu(4) × 2	3.3992(4)	Sb(2)−Lu(1) × 2	3.0596(9)
Lu(2)−Lu(1)	3.5512(5)	Sb(2)−Lu(2)	3.265(1)
Lu(4)−Lu(1) × 4	3.6852(5)	Sb(2)−Lu(5)	3.0808(7)
Lu(2)−Lu(3)	3.7861(7)	Sb(2)−Lu(2) × 2	3.0857(5)
Lu(2)−Lu(3)	3.9038(6)	Sb(1)−Lu(3) × 2	3.1870(4)
Lu(4)−Lu(2) × 8	3.3992(4)	Sb(1)−Lu(1)	3.3869(4)

polyhedra via common Lu3 and Lu2 atoms, respectively. The brown units about Sb2, approximately trigonal antiprismatic to Lu neighbors, interconnect green (Sb1) groups and share Lu1−Lu1 edges to generate zigzag chains around $^1/_4$, $^1/_4$, *z*, etc. The polyhedron about Sb1 (green) can be described as a trigonal prism $(Lu2, Lu3, Lu3)_2$ oriented along *z* that is unicapped by Lu5. Finally, Lu4 centers a parallel metal-rich region along 0, $^1/_2$, *z*, etc., with each Lu4 being eight-bonded within a rather distorted cube of Lu2 that shares faces down this projection. (Figure S4 shows this isolated polyhedron drawn in infinite projection to illustrate the distortions.) The 8-fold Lu4−Lu2 radial distances are a longer 3.40 Å here, and the Lu2−Lu2 edges of the rather distorted cube are either 3.26 or 4.02 Å in length. In contrast, the cube of Lu3 about the central Lu5 has radial separations (not drawn) comparable to those about Lu4, 3.45 Å, and cube edges that are in turn 0.4−0.5 Å longer. The anisotropic environment about Lu5 is likely responsible for its somewhat larger U_{33} value (Experimental Section).

The reported structure of Sc_7As_3[10] differs only qualitatively from the present one, principally in that it contains a split

position for the equivalent of Sc4, two atoms with 50% occupancy (and large U_{33} values) that are separated by 0.44 Å around the mirror plane at $z = {}^1/_4$. This disorder likely resulted because scandium within the distorted $(Sc2)_8$ cube (Figure 4, blue) is relatively too small. Correspondingly, the reported Sc4−Sc2 distances of 3.06 and 3.34 Å compare with Pauling's single bond metallic distance of 2.88 Å,[25] a value that would probably correspond to an unreasonably high bond order in this situation.

The overall structures illustrated here achieve to amazing degrees rather regular (and therefore presumably efficient) packing of two types of atoms for these stoichiometries, examples that maximize the more polar Tm−Sb or Lu−Sb interactions and at the same time give close and fairly regular packing of Tm/Lu atoms with many like neighbors that support delocalized metallic bonding among these. Although the numbers are an oversimplification, there are formally 6 or 12 excess electrons per Tm_3Sb or Lu_7Sb_3 (beyond the requirements of Sb^{3-}) in a "metallic" role, corresponding to 2.0 or 1.7 electrons per metal atom, respectively.

Acknowledgment. The authors thank Bin Li for some refinement checks. This work has been supported by the U.S. National Science Foundation, Solid State Chemistry, via Grant Nos. DMR-0129785 and -0444657 and has been performed in facilities of the Ames Laboratory, U.S. Department of Energy.

Supporting Information Available: Two files in CIF format and one PDF file containing three additional figures of the structures and magnetization data for Tm_3Sb at 2 and 300 K. This material is available free of charge via the Internet at http://pubs.acs.org.

IC0619409

(25) Pauling, L. *Nature of the Chemical Bond*; Cornell University Press: Ithaca, NY, 1966; p 403